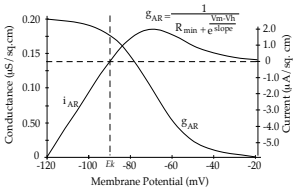

Dendritic Morphology, Inward Rectification and the Functional Properties of Neostriatal Neurons

Charles J. Wilson,
Department of Anatomy and Neurobiology University of Tennessee, Memphis

In: Single Neuron Computation T.McKenna, J. Davis and S.F. Zornetzer (eds), Academic Press, San Diego, pp. 141-171, 1992.

INTRODUCTION

Recent advances in cellular neurophysiology have revealed a wealth of very nonlinear membrane properties that greatly enrich the landscape of possible neuronal computation. At the same time, the complexity introduced by these nonlinearities has made the task of analyzing their functional properties enormously challenging. With relatively simple linear systems it is a reasonable strategy to attempt a complete description of the dynamic behavior of the system that can be used to predict the output for any input signal. Given the complexity and nonlinearity displayed by neurons, it may be expedient to use a less ambitious strategy, restricting the analysis to a limited set of inputs that are already known to be important for the operation of the system. To the experimental neurobiologist, the most natural approach is to ask what new computational capability is introduced when a particular ion channel is inserted into the membrane of the neuron, or a new synapse is attached to its surface. The problem is less straightforward than it sounds, however, because the functional impact of new inputs or new membrane properties is strongly dependent upon the nature of the input signals and interactions with other membrane nonlinearities. In the absence of a more general solution, it may be best to examine specific neurons with their own characteristic sets of nonlinearities, arrangements of inputs, and patterns of afferent activity. The computational facilities endowed upon those neurons by particular nonlinearities can then be examined in their natural setting. This increases the likelihood that the results will fall in a relevant part of the complicated parameter space that represents the potential interactions of large numbers of inputs with all possible manner of nonlinear synaptic and membrane properties.

The spiny projection neuron of the neostriatum is a good candidate for this kind of analysis. The neostriatum and related structures represent a large proportion of the forebrain, second only to the cerebral cortex itself. Understanding the role of the neostriatum in the context of the overall organization of the brain requires a knowledge of the transformation applied by the neostriatum upon its input. This is especially critical because the roles of the neostriatum in experience and behavior are somewhat obscure, or at least not as well understood as those of the cortical regions which give rise to its input fibers. By studying the modifications of cortical signals that occur as they traverse the neostriatum, we can expect to gain information of fundamental importance on the functional properties of this prominent region of the brain. In addition, the neostriatal projection neuron shares many of its morphological and physiological characteristics with cells in a variety of other regions of the forebrain, and it is likely that the principles that govern its function will be similar to those other neurons.

Like the cerebral cortex, the neostriatum contains a very large number of neurons whose axons exit the nucleus, and which differ according to the target of their axons. Although there are several different types of cells known to be present, the majority of the neurons are of one morphological type characterized by its long axon and spine-laden dendrites and called the spiny projection neuron (e.g. DiFiglia et al., 1976, Chang et al., 1981). Among these cells there are a number of subtypes, but they do not differ greatly in either their overall morphological features, or in their physiological properties (Kawaguchi, et al., 1990a; 1990b). The electrical properties of these neurons, their anatomical connections, and their cellular morphology have all been studied and described in some detail. Importantly, these same cells receive the majority of synaptic inputs from afferent fibers. Thus the circuit consisting of the spiny projection neurons and their afferent fibers comprises the simplest and the numerically predominant through–pathway for information entering the neostriatum. The computation that can be performed by a single neuron in this circuit is the fundamental functional operation of the neostriatum.

Firing Pattern of Neostriatal Spiny Projection Neurons:

The firing pattern of the spiny projection neurons is characterized by episodes of firing separated by long periods of silence. In animals deeply anesthetized with barbiturates, practically no spontaneous firing can be observed at all. In awake animals, episodes of spontaneous activity are associated with the initiation and execution of planned or learned movements (e.g. Evarts et al., 1984). Intracellular recording experiments in unanesthetized animals (Hull et al., 1970; Wilson and Groves, 1981) and in lightly anesthetized animals (Sedgwick and Williams, 1967; Calabresi et al., 1990) have shown that firing during these episodes arises from periods of sustained (0.1-3 sec) membrane depolarization. Separating these periods of depolarization are longer episodes of membrane hyperpolarization and greatly decreased synaptic noise. An example showing this firing pattern, and the underlying membrane potential changes is shown in Figure 1. The transitions between the depolarized and hyperpolarized states underlie the pattern of action potentials generated by the striatal neuron, and the patterns of firing of neurons in their target structures, the globus pallidus and substantia nigra.

Distribution of Synaptic Inputs on the Spiny Projection Neuron:

Afferent inputs to the spiny projection neurons terminate mostly on the dendrites, with more proximal inputs arising from interneurons within the nucleus. The structural features of the neostriatal spiny neuron are well known from studies using intracellular staining, as well as the classical Golgi technique. An example of the dendritic and local axonal arborizations of a spiny projection cell is shown in Figure 2, as reconstructed from serial sections through an intracellularly stained cell. Somatic diameter ranges from 10 to 15 μm, and the dendritic tree fills a volume ranging from 250-500 μm in diameter. Twenty to thirty dendrites arise from approximately half that number of short spine-free dendritic trunks which branch within the first 20-30 μm to give rise to less branched, gradually tapering dendrites that are densely covered with dendritic spines. The local axonal arborization usually stays in the general vicinity of the dendritic field. Electron microscopic studies have shown that the synapses made by the axons are primarily on the somata, dendrites and dendritic spines of other spiny projection neurons (Wilson and Groves, 1980).

An adequate representation of the morphological features of the neuron requires information that is not available in the light microscope. The dendrites are of small caliber (on the order of 1 μm) at their origin, and become very fine at their tips. Accurate estimates of dendritic surface area cannot be obtained in the light microscope, both because the measurement of diameter is not

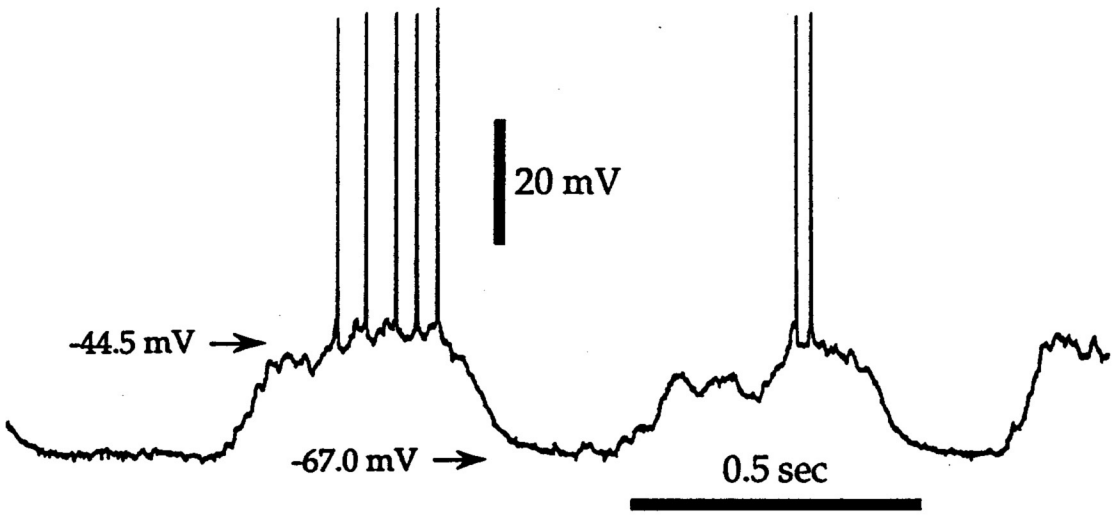

Figure 1. Spontaneous membrane potential fluctuations of a neostriatal spiny neuron, and the spontaneous firing pattern caused by those fluctuations in an animal anesthetized with urethane. Noisy depolarizing episodes arise from a hyperpolarized baseline with relatively little spontaneous noise. Action potentials arise from membrane potential fluctuations that are superimposed upon the depolarizing episodes. Transitions between the depolarized and hyperpolarized states are abrupt, and occur at irregular intervals.

sufficiently accurate, and because the dendrites are not cylindrical in cross section. The dendritic spines have cross sectional diameters on the order of 0.1 µm, making estimation of their surface area even more problematical. Even the density of dendritic spines cannot be accurately judged from the light microscope, as they lie so closely together that they often fall into each others' circles of confusion.

More accurate estimates of the distribution of membrane on the neostriatal neuron have been made using electron microscopy of thin sections, and a more specialized technique, high voltage electron microscopy (HVEM) of thick (3-5µm) sections (Wilson, 1983). An example showing the improved resolution gained by the HVEM technique is shown in Figure 3. Intracellular staining is responsible for nearly all the contrast in the image, as it is with light microscopic examination, and so the image can be interpreted in exactly the same way as it would be in the light microscope. The resolution is approximately 50 times that of the light microscope, however, allowing for very accurate measurement of somatic and dendritic diameters, spine densities and the dimensions of dendritic spines. Because the stained neurons used for HVEM analysis are also visible in the light microscope, systematic sampling of different parts of the dendritic tree, required for quantitative analysis, is a simple matter. Analysis of spiny neurons using this technique has allowed accurate measurement of the linear dimensions of the cells, but because dendrites are not made up of symmetrical components such as cylinders and spheres (this is obvious from examination of the cell in Figure 3), surface area cannot be estimated from these measurements in a straightforward manner. Systematic sampling and serial electron microscopic reconstruction of samples from the dendrites have provided corrections that can

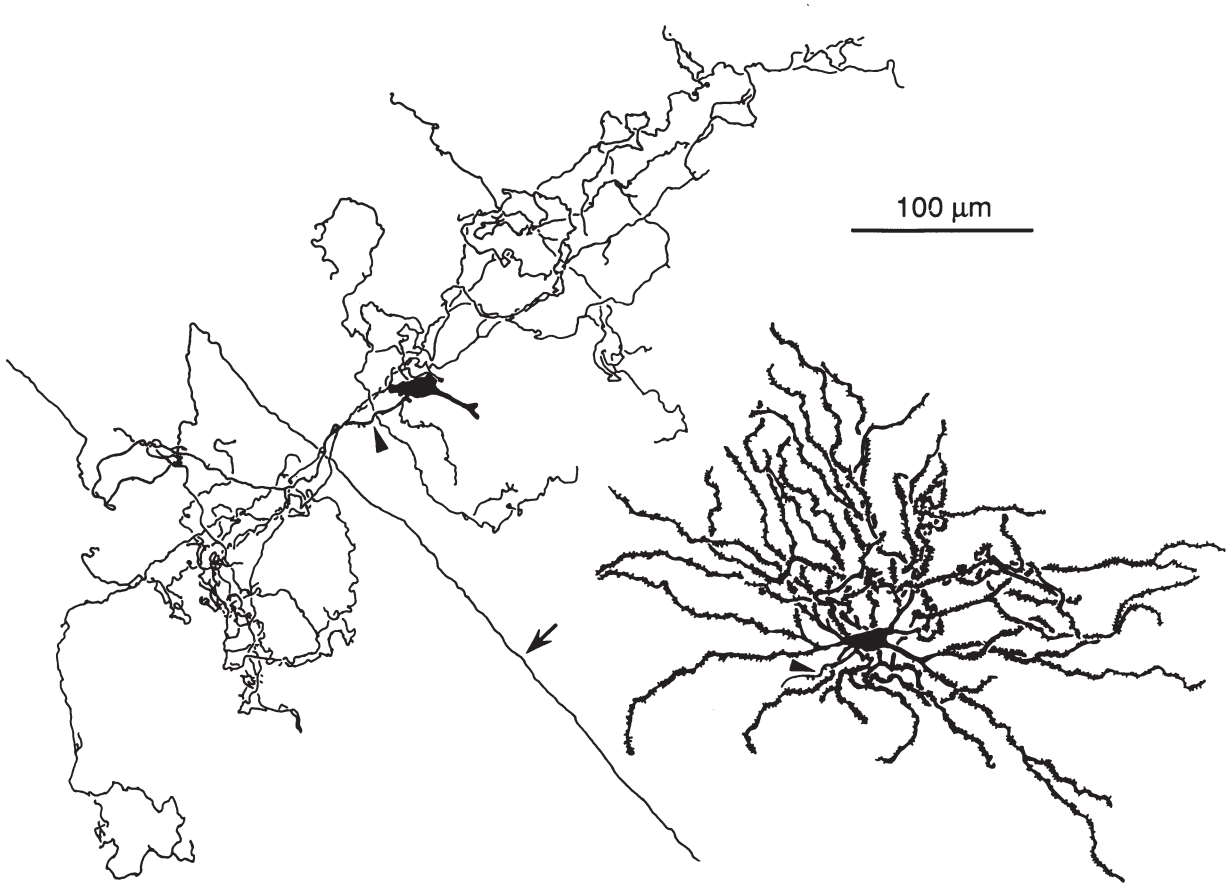

Figure 2. Reconstruction of the dendritic and local axonal arborizations of a neostriatal spiny neuron stained by intracellular injection of biocytin. The initial segment of the axon is indicated by an arrowhead, and the main axonal branch is indicated by the arrow. After emitting the local collaterals, the axons of these cells descend through the internal capsule bundles to innervate the globus pallidus, entopeduncular nucleus and substantia nigra. From Kawaguchi et al. (1990b).

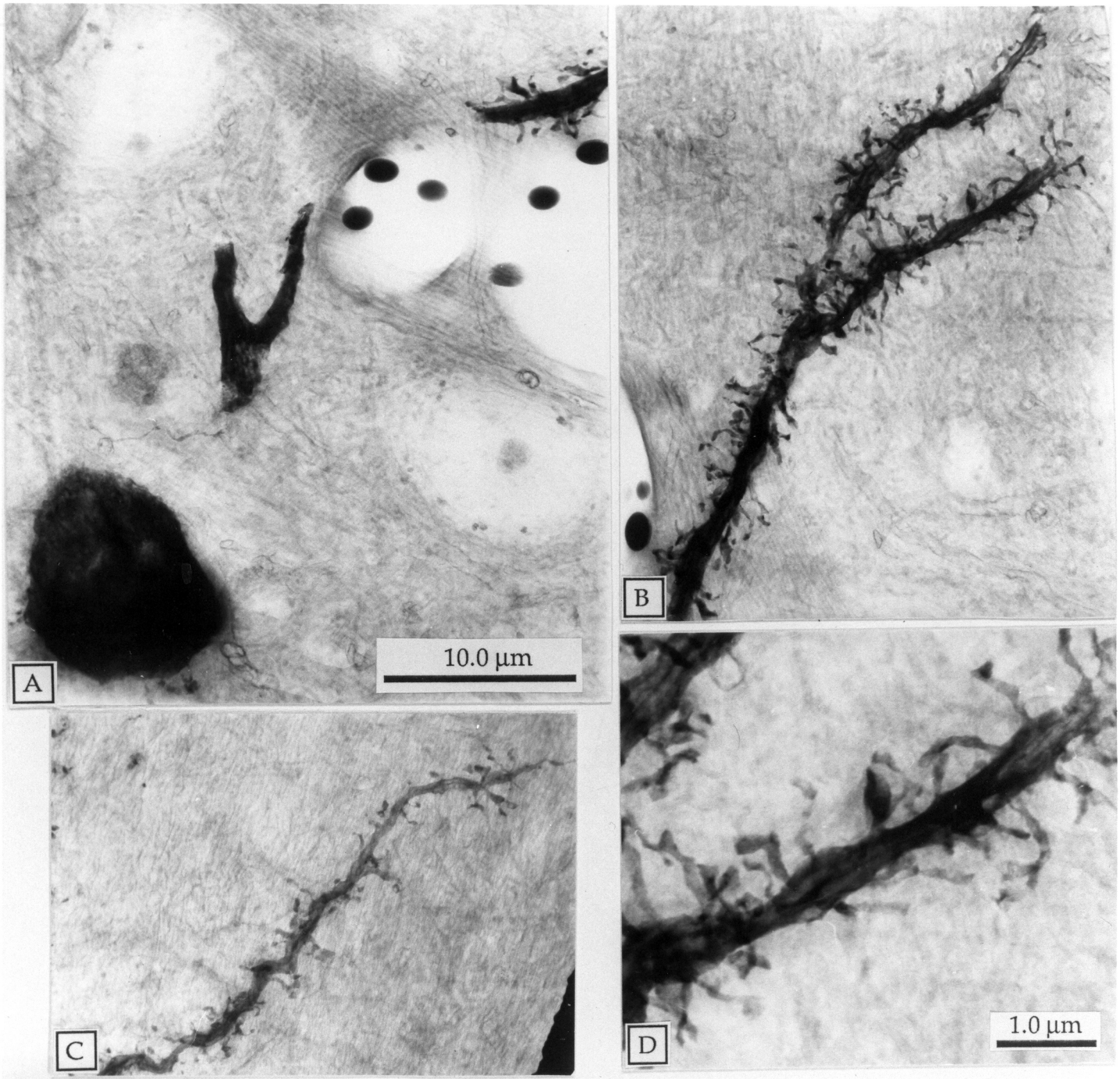

Figure 3. High voltage electron micrographs showing the morphological features of neostriatal spiny projection neurons at high resolution. The neuron was stained by intracellular injection of horseradish peroxidase, and prepared for examination in the HVEM as described previously (Wilson, 1987). Section thickness is 5 µm. A. The soma, a portion of the aspiny initial part of a dendritic tree with a branch point, and a part of the spiny part of the same dendritic tree are shown. The soma was only partly contained in the section, but was sectioned through its center, so its apparent diameter is representative of spiny neurons. The diameters of the aspiny part of the dendrites, and their non-cylindrical shapes are evident. B. A segment of dendrite taken from the most densely spiny region of the dendritic tree. The high density of spines and the variety of their shapes is evident, as is the irregular dendritic countour. C. A dendritic tip from a spiny neuron, shown at the same magnification as in A and B. Note the reduced spine density and rapid tapering of dendritic diameter. D. High magnification view of a portion of the densely spiny dendrite shown in B, to illustrate the high resolution available in the HVEM for measurement of dendritic spine shapes. The texture of the background tissue is due to treatment of the section with osmium tetroxide.

be applied to the HVEM measurements to yield more accurate surface area estimates (Wilson et al., 1983). Although very reliable, this approach requires three different kinds of data using three different microscopic techniques, and is expensive in time and effort. A more direct route to surface area measurements has been introduced recently, using axial tomographic reconstruction of dendrites from series of HVEM images taken over a range of specimen tilt angles. This technique has not yet been systematically applied, but in a preliminary test it yielded estimates of spine and dendrite surface area that closely matched those obtained previously from serial section data (Mastronarde et al., 1989).

A Model of the Spiny Neuron:

The distribution of surface area on the neostriatal spiny neuron as estimated using the combination of light, HVEM and conventional electron microscopy is shown in Figure 4. Rather than the distribution of surface area for a single neuron, this is a composite based on microscopic analysis of many neurons. The surface area is combined for all the dendrites, and is expressed in square micrometers per micrometer of dendritic length as a function of distance from the soma. The total dendritic surface area decreases with distance from the soma because of the tapering of the dendrites and the sparse branching of their arborizations. The surface area due to dendritic spines increases rapidly between 20 and 50 µm from the soma, and this reflects the changes in spine density that occur over this region in the dendritic field. Spine density tapers off gradually toward the tips of the dendrites, and this is reflected in the surface area as well. None of the variation of spine surface area is due to any systematic change in spine shape on the neurons. Despite great variation in the shapes and sizes of dendritic spines as seen in electron micrographs of striatal neuropil, these features were not found to be correlated with position on the dendritic tree (Wilson et al., 1983).

In the model used for the simulations, the surface area represented in Fig. 4 was distributed onto 6 identical dendritic trees, each of which branched twice. The first branch was placed 10 µm from the soma, in the spine–free portion of the dendrites, and the second at 30 µm from the soma, in the first part of the spiny portion of the dendritic field. The model of the cell thus had 24 dendritic tips. Spine density distribution was based on a HVEM correction of counts of the mean spine density from 5 neurons whose spines were counted in an earlier study (Wilson et al., 1983). It was maximal at a distance of 50 µm from the soma, where there were 3 spines per micron of dendrite, and tapered in an approximately linear manner to a value of 0.6 spines per micron at the dendritic tip. The primary dendrites were 10 µm long tapered cylinders with diameters of 2.25 µm and no spines, the secondary dendrites were 20 µm long, with a diameter of 1.0 µm initially and tapering to 0.96 µm. The tertiary dendrites were 190 µm in length, and their diameters were tapered from 0.63 µm at their origin to 0.29 µm at the tips using data from HVEM analysis. Dendritic spines not activated synaptically had a mean surface area of 1.46 μm^2,corresponding to the mean value determined from serial section electron microscopic analysis (Wilson et al., 1983). Synaptically quiet spines in the simulations were represented by increasing the membrane capacitance and conductance of the dendritic segment attached to the spine by an amount that represented the increased surface area associated with

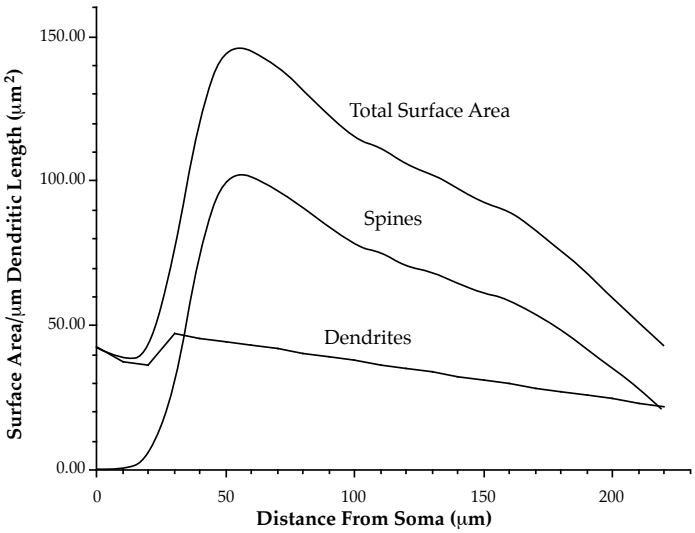

Figure 4. Surface area profile of the neuronal model used in the simulations. This profile was based on the average dendritic spine surface areas measured from serial section electron microscopic analysis, spine density and dendritic diameter data obtained from HVEM analysis of intracellularly stained neurons, and dendritic branching data obtained using the light microscope. The surface areas do not represent any one neuron, but a composite of the spiny projection neurons analyzed in a number of experiments. The dendritic branching patterns have also been simplified so that all the dendritic trees arising from the soma are identical.

the spine. Detailed simulations of charge redistribution in the limited environment of an active synapse in a segment of dendrite showed that this approximation was accurate for the dimensions used for the spiny neuron and the time course of its synaptic conductances used in these simulations. Synaptically activated spines were represented using one isopotential compartment to represent the head, and three compartments to represent the spine neck. Dimensions of these spines were varied over the range found in striatal spiny neurons.

Input Resistance and Electrotonic Length of the Passive Model:

Although much is already known about the electrical characteristics of distributed neuronal membrane, the large contribution of dendritic spines to the dendritic surface area in spiny neostriatal neurons deserves some analysis as a basis for comparison with the same neuron after addition of the anomalous rectification conductance. Figure 5 shows the input resistance and electrotonic dendritic length of this model as a function of membrane resistivity. To illustrate the effect of dendritic spines on these parameters, a model of the neuron without dendritic spines is compared with the results for the spiny dendrites. These results show that the additional surface area represented by dendritic spines greatly reduces the input resistance of the neuron at any value of membrane resistivity. Likewise, the additional dendritic surface area is added without any additional increase in the cross sectional profile of the dendrite available for longitudinal current flow. Thus the spines act to reduce membrane resistance of the dendrite without reducing the axial resistance. This is similar in effect to a decrease in the membrane resistance that occurs with no alteration of membrane time constant (as described earlier). The effective electrotonic length of the dendrite is increased by the presence of dendritic spines, as would happen if membrane resistivity were reduced. This effect is very pronounced when the membrane resistivity is low, but continues to be felt even with very high membrane resistivity.

The range of input resistances and electrotonic lengths normally attributed to spiny neurons in neurophysiological experiments (Kita et al., 1984; Bargas et al., 1988) are shown using dashed lines (Fig. 5). One remarkable feature of these

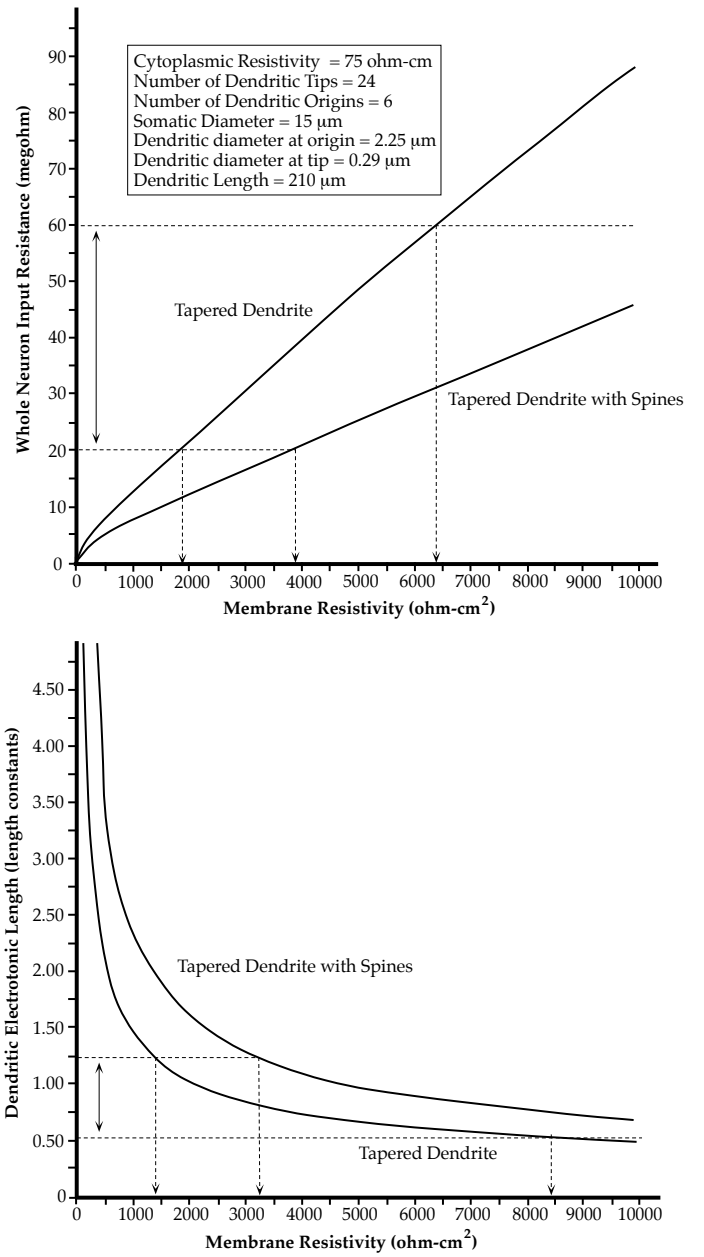

Figure 5. Effect of dendritic spines on the steady state parameters of the neuron model. In the upper graph, input resistance is shown as a function of membrane resistivity for the neuron model with and without dendritic spines. The range of input resistances usually reported for spiny projection neurons, and the corresponding membrane resistivity values are indicated by dotted lines. In the lower graph, dendritic electrotonic length is shown as a function of membrane reisitivity for both neuron models. Again, the range of reported values for spiny projection neurons is shown with dotted lines. The presence of dendritic spines greatly lowers the input resistance and raises the dendritic electrotonic length expected at any value of membrane resistivity. Likewise, the membrane resistivity predicted from estimates of these parameters is increased several fold due to the presence of spines on the neurons.

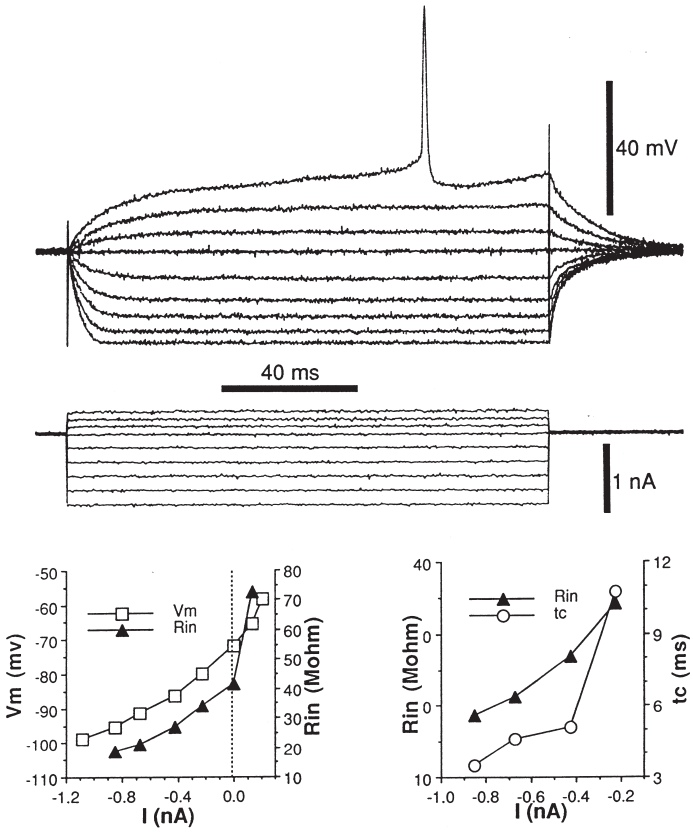

Figure 6. Responses of a striatal spiny projection neuron to intracellularly applied current pulses, and the variation of input resistance and time constant as a function of the amplitude of the injected current. In the upper panel, the range of current pulses and transients are shown. In the graph at the lower left, the steady state membrane potential is plotted against the amplitude of the current for all transients except the one evoking the action potential. The anomalous rectification is indicated by the curvature of this steady state current voltage relationship. This change in the steady state input resistance is indicated in the same graph. At the lower right, the variation in input resistance is superimposed on the change in time constant of the charging curve for each current step. The time constant was calculated from the late portion of the charging curve, in which the membrane potential was near its final value. The response to the most hyperpolarizing current step (in which a time-dependent anomalous rectification is evident) and the depolarizing responses were not used in this analysis to avoid confusion of the fast inward rectification with other voltage dependent currents. Data from Kawaguchi, et al. (1990a).

empirical data is their wide range. This variability from cell to cell can be seen to correspond with an even larger range of membrane resistivity, from about 3500 ohm-cm^2 to over 10000 ohm-cm^2. If the spines were not present, this same variability would correspond to a narrower range of membrane resistivity, between 1500 and 6500 ohm-cm^2, and the resistivity calculated from input resistances would make a much poorer match with those predicted from the measurement of electrotonic length. If the range of input resistances and electrotonic lengths observed in the neurophysiological measurements were due to differences in input resistivity among neurons, it might be expected from the curves in Fig. 5 that membrane time constant would vary even more, reflecting the very wide range of membrane resistivity. If the membrane capacitance were 1 µF/cm^2, the time constant might be expected to vary from about 3.5 ms to greater than 10 ms.

Effect of Fast Anomalous Rectification on Input Resistance and Time Constant :

A very fast anomalous rectification in neostriatal neurons has been described in most studies of the membrane properties of neostriatal neurons (Kita, et al., 1984; Calabresi, et al., 1987; Kawaguchi et al., 1990a). If this conductance could alter membrane resistivity over a wide range, it could be responsible for the range of observed values shown in Fig. 5. In a recent study of the membrane properties of neostriatal neurons in slices, Kawaguchi et al (1990a) measured the variation in input resistance and time constant over the normal range of membrane potentials. An example from the results of that study is shown in Figure 6. The very rapid time course of activation of the inward rectification is evident in the traces at the top of Figure 6. The non-exponential nature of the charging curves is evident in the responses to the large current steps, and from the asymmetry in the responses to onset and offset of the curves. The rapid response of membrane resistivity to changes in membrane potential can explain most of the features of these charging curves. Because the change in membrane resistivity follows changes in membrane potential very rapidly (i.e. much faster than the rate of decay of charge through the membrane resistance), the time constant may be considered to be varying continuously during the response to current. Thus deviation of the responses from an exponential curve are greatest in the first part of the transients when the rate of change of membrane potential is highest. The later parts of both the onset and offset transients are associated with smaller rates of change of membrane potential, and these segments of the response are very nearly exponential in form. If an exponential curve is

fit to the late portions of the responses to onset and offset of the response to current pulses in spiny neurons, as is the usual way of measuring the time constant of the cell, very different values are obtained depending upon whether the onset or the offset of the response is used. Fitting exponentials to the offset curves gives a single value for the time constant regardless of the amplitude of the current pulse. This time constant reflects the membrane resistivity at the resting membrane potential. If the time constant is measured from the late portion of the transient at the onset of a current pulse, the result depends very much on the amplitude of the current pulse. This is because the time constant obtained this way is measured at a membrane potential near the steady state value that will be achieved by the pulse, and so reflects the membrane resistivity of the cell at this membrane potential. Using the membrane potential responses to the onset of current pulses, it is thus possible to estimate the time constant of the neuron as a function of membrane potential. The input resistance can likewise be estimated (although somewhat less rigorously) by taking the slope of the steady state voltage-current curve at each voltage point. These measures of input resistance and time constant are shown for a spiny neuron in the lower part of Fig. 6. The time constant and input resistance of this one neuron could be made to vary over the entire range reported for the population of neostriatal neurons, simply by adjusting the membrane potential.

Because the anomalous rectification acts so quickly, it is permissible to continue to use the conventional model of the neuron, but with the membrane resistivity made a function of instantaneous membrane potential. The range of time constants and input resistances obtained from analyses of individual spiny neurons like the one shown in Fig. 6 can be compared with the input resistance curve in Fig. 5. This comparison suggests that the membrane resistivity of spiny neurons varies between about 3000 ohm-cm^2 and 20000 ohm-cm^2, over the rather modest range of membrane potentials from about -100 mV to -60 mV. These values were used to simulate the anomalous rectification of neostriatal spiny neurons using the model of the fast inward rectification described by Hagiwara and Takahashi (1974) for the starfish egg. The potassium equilibrium potential was fixed at -90 mV. This is important for the anomalous rectifier because

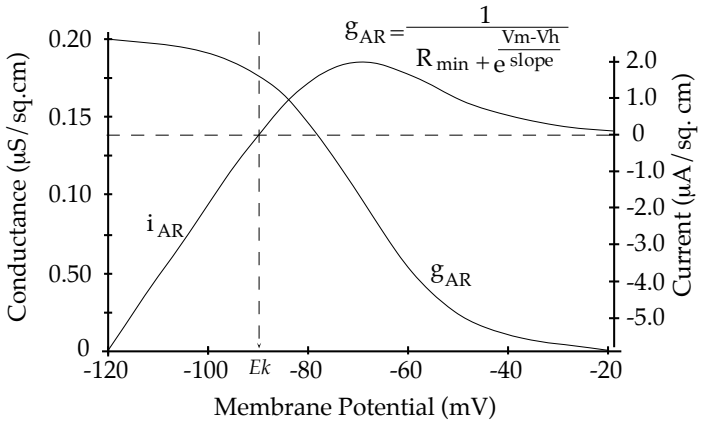

Figure 7. Activation curve for the inwardly rectifying conductance used in the model of the spiny neuron, and the equation used to generate it. Rmin determines the maximum conductance, while the shape of the activation curve is determined by the half-maximal voltage (Vh), the potassium equilibrium potential (Ek) and the slope factor (slope). The current density associated with this conductance is also shown.

the conductance, as well as the current, has been shown to be dependent upon the deviation of the membrane potential from E_k. The maximum conductance and the activation curve was varied somewhat in these simulations, and the curve best matching the input resistance and time constant data for neostriatal spiny neurons is shown in Figure 7, along with the current density associated with that conductance. Because the fast anomalous rectification approaches zero conductance as the cell is depolarized, a constant leak conductance (20000 ohm-cm^2) was placed in parallel with it, limiting the whole neuron input resistance (at the soma) to 60 megohm (not shown). A constant leak conductance of this type is probably not what determines the input resistance of neostriatal neurons when depolarized, but rather other voltage-sensitive potassium currents (see below). To prevent confusion with the effects of the anomalous rectifier, such currents were excluded from these simulations, however.

The effect of the anomalous rectification on the responses of the model cell to current steps is shown in Figure 8A (top). The characteristic asymmetry of the responses of neostriatal spiny neurons is evident in the simulated responses, as is the ramp-like depolarization that is seen with moderate depolarizing pulses. This almost linear ramp depolarization is caused by the positive feedback inherent in the anomalous rectifiication. Small depolarizations increase the input resistance of the neuron, thereby increasing the

depolarization caused by the constant applied current, which again raises the input resistance. This is active over the entire range of the activation curve for the anomalous rectification, and ultimately causes the membrane potential to saturate at a level determined (in these simulations) by the leak conductance. In a more realistic simulation, this limiting conductance would probably be due to voltage-sensitive potassium currents, and would be a complicated function of the recent history of membrane potential fluctuations (Surmeier et al., 1988; 1989; 1991). Over the range of membrane potentials used here, which did not engage the mechanism that limits the response to depolarizing currents, the current-membrane potential relation was a good match for that seen in spiny neostriatal neurons (Fig. 8, middle left). The same range of currents also reproduced the time constant variation observed in neostriatal neurons (Fig. 8, middle right). Like the time constant variation seen in neostriatal neurons, this was seen only in the responses to the onset of current injection, and the time constant obtained from the last portion of the transient was appropriate for the membrane resistivity at the asymptotic (steady state) level of depolarization of the neuron for each pulse. Time constants obtained from examination of the late portion of the transient to current offset were very nearly the same for all transients, and were appropriate for the membrane resistivity of the neuron at its resting potential.

If the Time Constant Is Not Constant, the Length Constant Isn't Either:

This variation in membrane resistivity implies that the electrotonic length of the spiny neuron may also vary between about 1.3 and 0.5 length constants over the same range of membrane potential (Fig.5). This could explain the apparent contradiction in the literature concerning both the time constants and length constants of spiny neostriatal neurons. In the first study of membrane properties of neostriatal neurons, performed by Sugimori et al. (1978) using cat neostriatum in vivo, the time constant of the neurons was reported to be about 15 ms, and transients recorded in response to current steps could be fit with a single exponential, suggesting that the dendrites were electrotonically too short to measure. In subsequent studies in slices of neostriatum, a range of dendritic lengths and time constants were observed, but generally the time constants were shorter, around 5 ms, and at least a second exponential decay could be detected in the responses to current steps (Kita et al., 1984; Bargas, et al., 1988). This discrepancy has been suggested to be due to species differences, or to the local potassium concentration, but a more simple explanation is suggested by these results. In the slightly more depolarized neurons of the in vivo cat neostriatum (with synaptic inputs intact), time constants are longer and dendritic lengths shorter than those obtained in slices.

In the simulations shown in Figure 8, electrotonic length was examined as a function of the injected current, using two approaches. Because of the non-cylindrical distribution of membrane and the nonlinearity of the membrane, the equivalent cylinder model cannot be guaranteed to yield an accurate estimate of dendritic electrotonic length from a decomposition of the transient into exponential components (Rall, 1977; Fleshman, et al., 1983; Durand, 1984; Kawato, 1985). Nonetheless, this analysis was performed on the transients, to estimate the error introduced by these deviations from the ideal case. For comparison, the effective dendritic length was also measured using the difference between the average response at the dendritic tips, and that at the soma, measured at the end of the 100 ms current pulses (Fig. 8 middle left). Because the response to the larger depolarizing currents had not achieved steady state at the end of the current pulse, this estimate was somewhat approximate. This failure to achieve steady state with depolarizing pulses is an essential feature of the model with anomalous rectification, and could not be avoided. The model will not achieve steady state until the current is limited by some additional mechanism (in this case the leak conductance). The same behavior is observed in intracellular recordings from neostriatal neurons (Kawaguchi et al., 1990a), but probably for somewhat more complicated reasons.

The variation in dendritic electrotonic length measured by peeling exponential components from the transient (calculated using Kawato's 1985 variant of Rall's method) was in reasonably close agreement with the values obtained using the steady state dendritic decrement (Figure 8 bottom) and both of them reproduced the entire range of dendritic lengths reported for

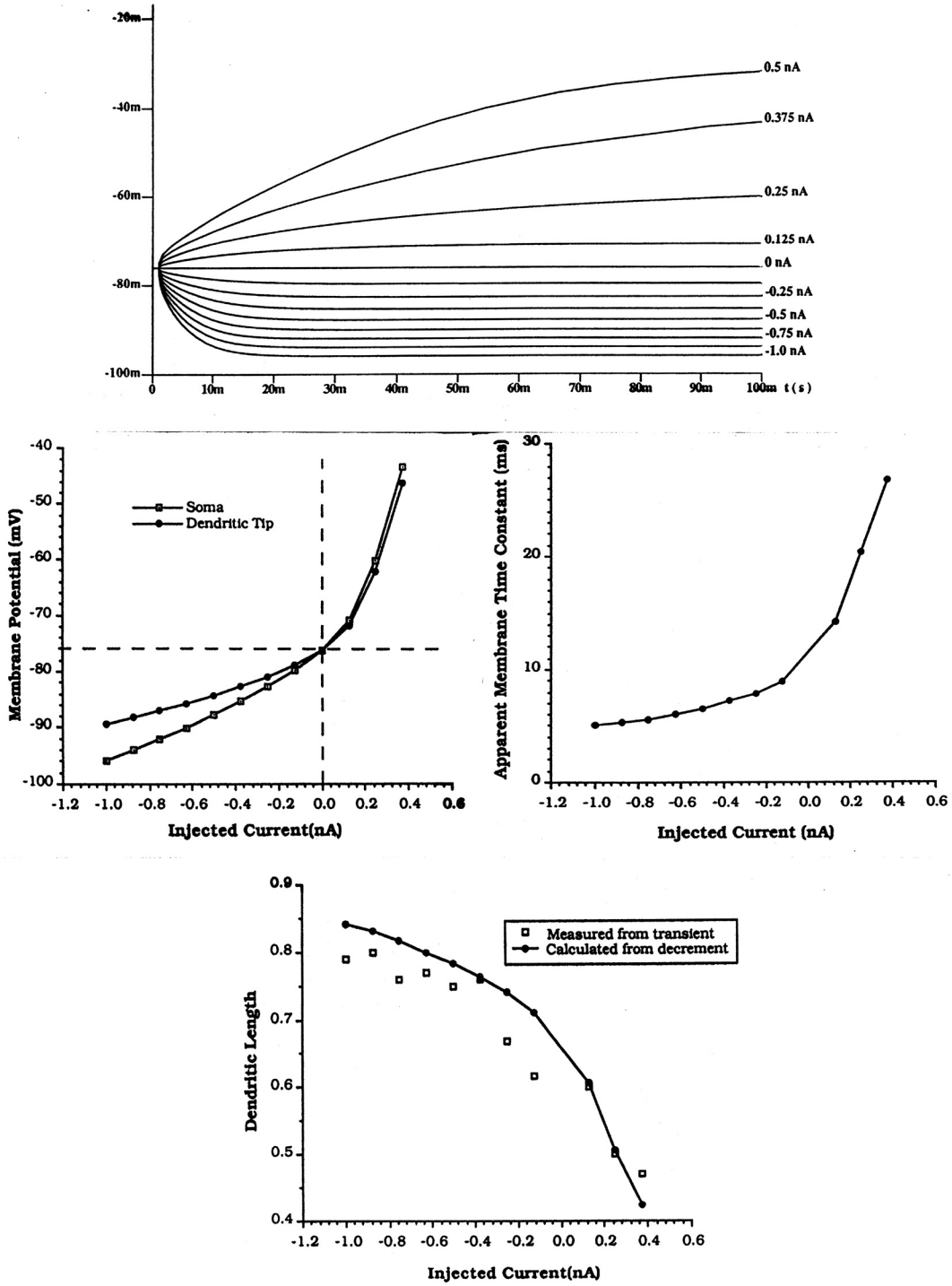

Figure 8. Responses of the neuron model to current steps. The graph at the top shows the transient response to somatic current steps of various amplitudes (amplitudes of currrent steps are shown at the right of each transient). The graph at the middle left shows the steady state membrane potential recorded both at the soma and at the tip of a dendrite. The effect of the inward rectifier on the somatic resistance matches that of the real neuron in Figure 6. The decay of voltage from the soma to the dendritic tip is also seen to be dependent upon the size of the current step. This is due to the change in electrotonic length of the dendrite as a function of membrane potential. This change is shown in the bottom panel. Dendritic length, calculated by peeling exponentials from the transient, is shown as a function of the size of the current step, along with the electrotonic length obtained from the steady state voltage difference between soma and dendritic tip. Both show a strong dependence on injected current, which is due to the variation of membrane resistivity with changes in membrane potential. At depolarized membrane potentials, the dendrites become electrotonically compact. Similarly, the membrane time constant (obtained from the last part of the transient response) is greatly lengthened when the membrane is depolarized.

neostriatal neurons in intracellular recording experiments. Thus the dendritic length of a neostriatal neuron may not be constant, but may vary from less than half of one length constant, to more than 1 length constant, depending upon membrane potential.

Synaptic Integration in the Spiny Neuron:

The variation of length and time constants of the neurons could also have profound effects upon synaptic integration in these neurons. Many excitatory synaptic inputs are located in the distal dendrites. When the dendrite is relatively polarized, due to an overall low level of excitatory input, the anomalous rectifier acts like a distributed shunting inhibition, reducing the input resistance, increasing the effective dendritic length, and reducing the time constant. These decrease the ability of excitatory synaptic inputs to sum effectively. If, however, enough inputs are active to depolarize the dendritic membrane somewhat, they can remove a portion of the conductance of the inward rectifier, and thereby increase their own effectiveness and that of any synaptic excitation arriving during the time course of the depolarization. The spatial extent of this cooperative effect among synapses would correspond to the spatial spread of the depolarization. One interesting feature of this mechanism is that it has the same time course and spatial domain as the classical synaptic nonlinearity, but it acts in the opposite direction. Synapses with similar actions are known to sum in a less than arithmetic way because of the classical synaptic nonlinearity, in which the voltage change generated by each synapse decreases the driving force for synaptic current at the others. Like the cooperative effect that might be expected to result from anomalous rectification, the synaptic nonlinearity is very fast in onset. It therefore can be though of as strictly dependent upon membrane potential.

To determine the effect of the synaptic nonlinearity and inward rectification when acting simultaneously, a simulation of synaptic activation of the model neostriatal spiny neuron was performed, comparing activation of large populations of synapses distributed in the dendritic tree in a neuron with and without the inward rectification. Because the placement of the synapses on dendritic spines, and the distribution of the synapses on the dendritic tree proved to be important influences on the results, the effects of these morphological parameters will be addressed first.

Dendritic Spines and Synaptic Strength:

Many theoretical studies have emphasized the potential role of dendritic spines in the regulation of synaptic strength (e.g. Diamond, Gray and Yasargil, 1970; Rall, 1974; Koch and Poggio, 1984; Perkel and Perkel, 1985; Wilson, 1985; Shepherd et al., 1985). In many of these, the dendritic spine is postulated to act as a series impedance to current flow from the synapse to the dendrite, and to thereby produce a very large local synaptic potential in the spine. This large local potential has different implications in the various models, but it always relies upon some nonlinearity of the postsynaptic neuron. If the nonlinearity is a fast voltage–gated inward current, the local potentials in spines are enough to trigger spikes in the spines that may propagate to other spines (e.g. Perkel and Perkel, 1985; Shepherd et al., 1985, Miller et al., 1985; Rall and Segev, 1988). If the nonlinearity is nothing more than the classical synaptic nonlinearity, it should act to decrease the effectiveness of the synapse by limiting synaptic current flow (e.g. Rall, 1974; Koch and Poggio, 1984; Kawato et al., 1984;Wilson, 1984). There are a variety of other possibilities, based on other kinds of membrane nonlinearities. The possible synaptic attenuation effect of the dendritic spine which arises from the classical synaptic nonlinearity has been emphasized in studies of neostriatal neurons, because it helps to explain why the cells are not continuously depolarized and firing due to the spontaneous activity in the thousands of afferent synapses that are formed onto each cell (Wilson et al., 1983). Computer simulations of dendritic spines in the size range observed in the neostriatum have shown that these may act to limit synaptic current and so attenuate synaptic inputs (Wilson, 1984). In such computer models, however, there is only a single synaptically activated spine on the neuron, and the effect of the spine on that synapse is studied. When this is done, the synaptic effect of an axospinous synapse can be seen to be attenuated, and to make a relatively small EPSP (<10 mV) in the dendrite, despite the presence of a very large (>40 mV) EPSP amplitude in the spine head. When the influence of this small synaptic input is seen at the soma, it is further diminished and appears appropriately small, for example, less than 0.1 mV.

In the model of the spiny neuron used here the spine density in the dendrites is often 2–3 , and occasionally reaches 4–5 per micrometer. An examination of the effect of anomalous rectification on synaptic transmission in this neuron requires some additional data on the linear model in the case of large numbers of active synapses. For example, if only 10% of synapses are active within the time period that allows their nonlinear interaction, there may still be as many as 5 active synapses active per 0.1 length constant of dendrite (about 25 µm at -90 mV membrane potential). The resulting dendritic EPSP may be as large as the EPSP in the spine head, and so might engage nonlinear properties in the dendrites as well as those in the spines, if these are present. As an extreme case, consider the case when all synapses are simultaneously active with identical synapses, on an infinitely long densely spiny neuron. Because the currents injected into the dendrite by each spine will be equal, each spine would behave as if it were placed on a short segment of dendrite terminated at each end with an ope circuit. The length of the segment of dendrite will be equal to the distance between dendritic spines. If this is very short (less than 1 µm in the example used here), the dendritic input resistance will be as great as that of the spine, and any special privilege of the spine in triggering voltage-sensitive nonlinearities may be lost (unless this privilege is gained by something more than simply the morphology of the spine).

Simulation of simultaneous activation of synapses clustered in one spot on the spiny neuron model showed that this effect occurs even with relatively low densities of activated spines. This is illustrated in Figure 9 (A&B). In this simulation, the dendritic spines were made to be rather long and thin (3.0 µm long and 0.1 µm neck diameter) and the synaptic conductance change rather short (a = 100), and high amplitude (peak conductance 1.0 nS). This combination favors the current attenuation effect of the dendritic spine simulation, and produced an approximately 50% attenuation of the synaptic potential as seen at the soma when compared with an axodendritic synapse at the same location (Fig. 9B, traces marked *passive*). The active spines were placed 120–140 µm from the soma. This 50% attenuation was obtained when only one synapse was tested in isolation. Additional synapses were then synchronously activated within ±10 µm (~0.05 length constants) of that active synapse, and the effect of those other inputs on the effectiveness of the original one was examined. The effect of clustered synchronous activation on the peak amplitude of the composite synaptic potential, as it appeared locally in the dendrite, and as it appeared in the soma, is shown in Figure 9A. The current attenuation effect of the dendritic spine depends upon the existence of a large difference between the input resistances at the spine head and the dendrite. Thus, the current injected by the synapse cannot move the dendrite as near the reversal potential of the synapse as can the current injected at the higher resistance site at the spine head. Figure 9A shows, however, that clustered synaptic activity can depolarize the dendrite very effectively, and thereby reduce the proportional difference between axodendritic and axospinous synaptic inputs. This is clearly seen in Figure 9B, which shows the EPSP contribution per synapse as a function of the number of synapses active. The effectiveness of axodendritic and axospinous synapses approach each other quickly as the number of active synapses approaches 1 per µm of dendrite (only about 25% of the spine density at 80 µm from the soma of the spiny neuron).

It is not yet known exactly what proportion of afferent synapses are active on one neostriatal spiny neuron at any one moment. This is not because we do not know the firing patterns of the afferent neurons in the cortex, thalamus and elsewhere. It is because we do not know the divergence of these pathways in the neostriatum. Thus we do not know how many different afferent neurons contribute synaptic input to each neostriatal cell (although there are indirect arguments for the number being quite large). Similarly, we do not know the degree of correlation in the firing patterns of those cells whose influences do converge in the neostriatum. However, these simulations do not support the view that there is a very high level of synaptic input which is attenuated simply by the electrotonic properties of the dendritic spines. If the level of activity in converging afferents is more than a few percent, the effect of these synapses must be weakened by another mechanism.

Effect of Fast Anomalous Rectification on Synaptic Integration:

The result of adding the fast anomalous rectification to the simulation of spatially clustered synaptic input is evident in

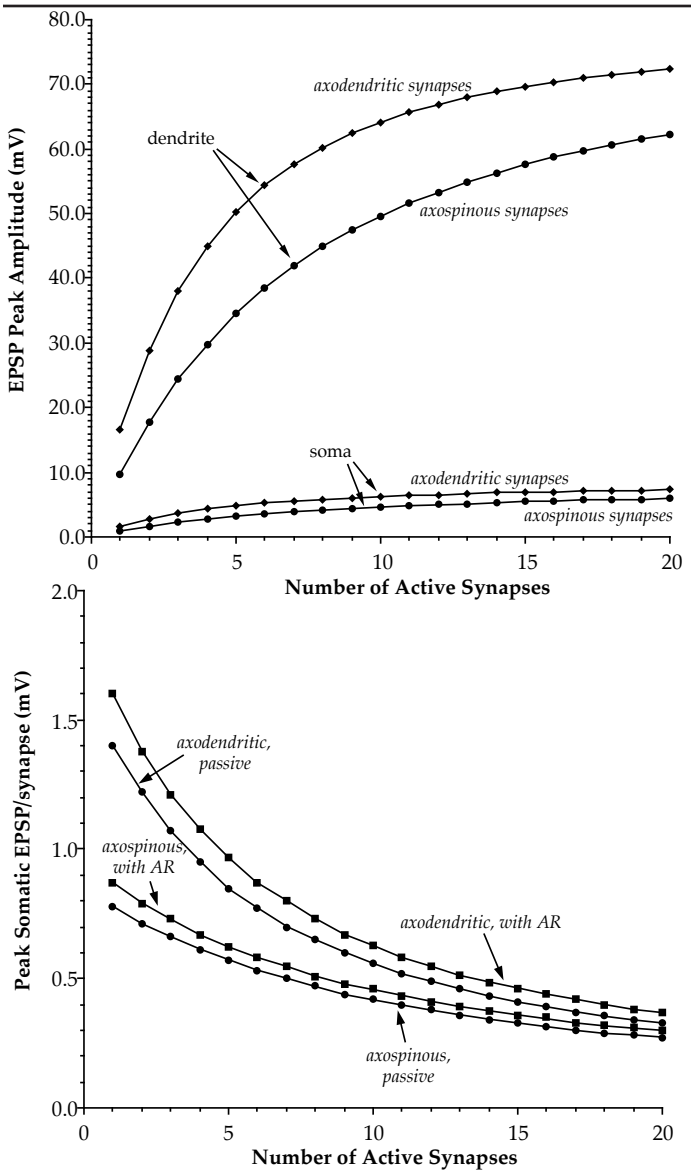

Figure 9. Integration of spatially clustered synaptic input on the model neuron. The peak amplitude of the EPSP evoked by synchronous activation of varying numbers of synapses along a single 25µm segment of dendrite on one dendrite of a model neuron is shown in the upper graph. The two upper curves show the amplitude of the local EPSP in the dendrite at the level of the synapses. Anomalous rectification has little effect on these curves, and so only the ones from the model with the inward rectifier are shown. The two lower curves show the resulting somatic EPSPs. Axodendritic synapses lead to larger local and somatic EPSPs, but the proportional difference between axodendritic and axospinous synapses decreases as the number of active synapses increases. This reduction in the difference between axospinous and axodendritic synapses as the synaptic density increases is more clearly shown in the lower graph, in which the somatic EPSP contribution of a single synapse is shown as a function of the total number of active synapses in the cluster. As the dendritic EPSP grows due to summation of EPSPs, it becomes large enough to engage the synaptic nonlinearity that attenuates synaptic current in the axospinous synapse. Addition of the inwardly rectifying nonlinearity has little effect on these differences because the local EPSPs in all cases are large enough to drive the local membrane into its high resistance region.

Figure 9B. In this simulation, the passive neuron had a membrane resistivity near the low end of the range for spiny neurons (5000 ohm-cm^2). The anomalous rectification simulation allowed a voltage-dependent variation of membrane resistivity between 3500 and 10000 ohm-cm^2, matching that of the simulations shown in Figure 8. Because local EPSPs (at the site of the synapse) were always large enough to engage the membrane resistance increasing effect of the anomalous rectification, the membrane in the dendrite had an effectively higher resistivity in the anomalous rectification model. The result of this was an increased length constant in the synaptically activated dendrite, and more effective spread of synaptic current to the soma. Thus, the synaptic effectiveness for the anomalous rectification model in Figure 9B is generally higher than that for the passive model. This is not a very important effect of anomalous rectification. Of course, the comparison would have been more realistic if the passive neuron had had an input resistance at the high end of the range, as the fast anomalous rectification in neostriatal neurons is probably due to an increase in potassium conductance with hyperpolarization rather than a decrease in membrane conductance caused by depolarization (e.g. Hagiwara and Takahashi, 1974). In any case, this simply shifts the curves vertically, and the addition of anomalous rectification has little or no practical effect on the function of the dendritic spine or the removal of the current attenuation effect of dendritic spines with clustered synaptic excitation.

When synaptic inputs are distributed on the dendrites, addition of anomalous rectification to the neuron model might be expected to have a larger effect. In this case, synaptic inputs produce more modest depolarizations throughout the dendritic tree, increasing the membrane resistivity in a general fashion. This might have the effect of reducing the electrotonic extent of the dendritic tree, and so the synapses could act in a cooperative way over a range of membrane potentials that correspond to that for the voltage sensitivity curve of the anomalous rectification. This possibility was tested by simulating synaptic excitation distributed uniformly in the dendritic field, and adjusting the density of this

excitation. To correct for the effects of synaptic location when only a few synapses were active, the results for a number of different randomly selected locations were averaged. The results of these simulations are shown in Figure 10. The synaptic effectiveness obtained with a single synapse is less in this simulation than in Figure 9 because a smaller conductance change was used (peak = 0.5 nS), and because the effective location on the dendrite is slightly more distal (the datum in Fig. 10 for 1 synapse is an average of many simulations at different dendritic locations). In the absence of the fast anomalous rectification, distributed synaptic inputs interfered destructively, but more weakly than in the case of clustered synaptic input. As in the case of clustered synapses, increasing the number of synapses active decreased the average effectiveness of any one, because the depolarization of the neuron moved all of the postsynaptic sites nearer to the reversal potential for the synapses. The degree to which this occurred was closely related to the membrane potential achieved during the synaptic activation, as can be appreciated by comparing the curves in Figures 9 and 10. But this depolarization, and the decrease in synaptic strength, occurs over a much larger scale. While synaptic strength was decreased to less than half with 10 active synapses when clustered, more than 250 distributed synapses were required to get the same decrement in synaptic strength. With such a large number of active synapses, the somatic depolarization is several times greater than that achieved by clustered synaptic inputs.

These simulations of the passive neuron suggest that despite the extended nature of the dendritic field and the low input resistance of the spiny neuron, only a small fraction of its inputs (perhaps less than 10%) may be required to depolarize the neuron to the tonic level usually observed in vivo (about 15-20 mV above

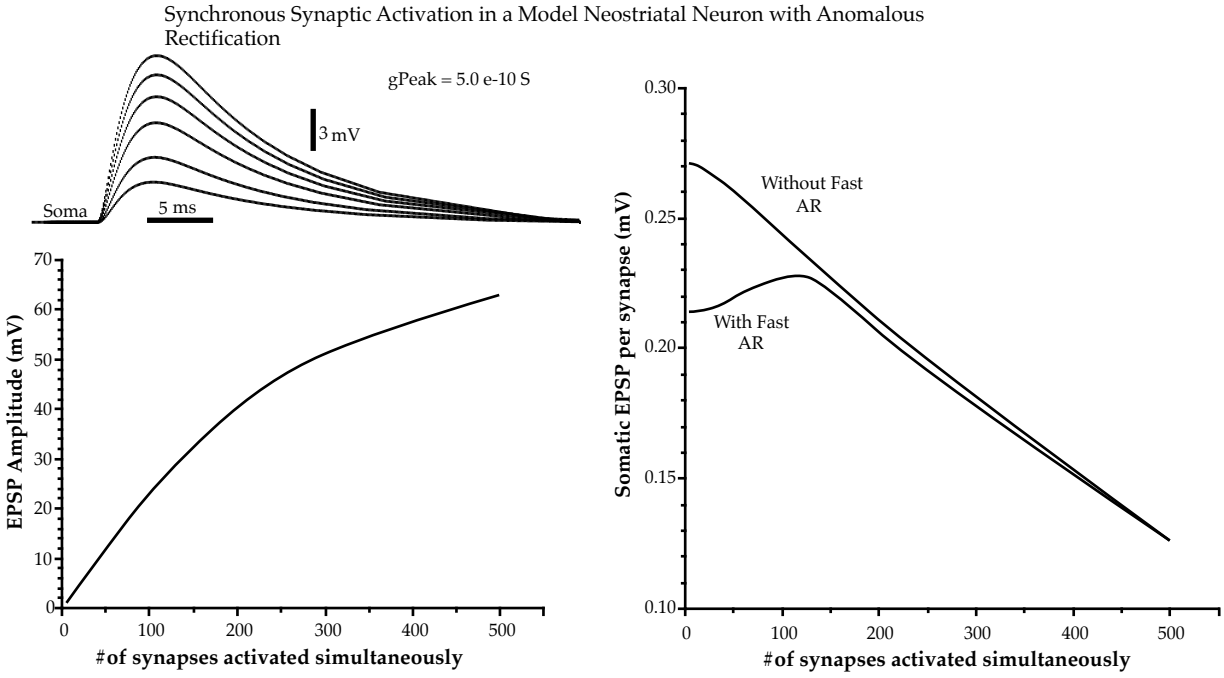

Figure 10. Integration of spatially distributed synaptic input on the model neuron. Synapses were activated at very low density uniformly over the surface of the spiny neuron model. At low values of synaptic density, points represent an average of responses obtained with synapses placed at various regions of the dendritic field. The traces at the upper left show the somatic EPSP obtained with varying numbers of active synapses. The graph at the left shows the peak somatic EPSP as a function of the number of simultaneously active synapses. Note that the somatic EPSP grows more linearly with the number of synapses than it does with clustered synaptic inputs. This is due to the deemphasis of the synaptic nonlinearity when synapses are distributed on the neuron. The somatic EPSP contribution of one synapse is shown as a function of the total number of active synapses in the graph at the right. Synaptic effectiveness in the linear neuron model decays more slowly with numbers of synapses than in the clustered synapse case. When the inward rectifier is added to the neuron model, an increase in synaptic effectiveness is seen with low synaptic numbers, and a maximal synaptic effectiveness is observed when approximately 150 synapses are active at the same time. This number of synapses depolarizes the soma by about 30 mV, and so corresponds roughly to the size of the depolarizing episodes, as seen in Fig. 1.

the resting potential for the membrane). They also show that the most effective distribution of these synapses is the most uniform possible one, with synapses placed as far apart as possible.

Addition of anomalous rectification to the neuron in this simulation had a profound effect on synaptic effectiveness. When few synaptic inputs were active, the membrane remained relatively polarized despite the synaptic activation, and it remained in its low resistance state. Somewhat larger groups of distributed synaptic inputs could lift the membrane slightly into the higher resistance state, decreasing electrotonic decay and so boosting effective synaptic strength as seen from the soma. Because the half activation voltage for the anomalous rectification is much nearer the baseline membrane potential than is reversal potential for the synaptic potential, the cooperative effect produced by such moderate depolarizations can overcome the opposite influence exerted by the synaptic nonlinearity. Thus in the curve showing synaptic strength in the case of a model neuron with fast anomalous rectification in Figure 10, increasing the number of active synapses produces an initial increase in synaptic strength. When the number of synapses becomes great enough to produce larger EPSPs and the effect of the anomalous rectification becomes maximal, the trend reverses, and the synaptic nonlinearity again undermines synaptic strength. This did not occur in the case of clustered synaptic inputs because of the large size of the local synaptic input (which turned the inward rectifying conductance off and raised the input resistance locally to its maximum) and the small region of the dendritic tree that was affected. The regions of the neuron that were not involved in the synaptic events remained mostly in the low input resistance voltage region, and the EPSP was degraded by electrotonic decay.

This effect of anomalous rectification on the strength of distributed synapses resembles a bandpass filter, in which synapses are most effective if they arrive in concert with a limited number of others. The peak of this curve, that is the preferred number of simultaneous synapses, is determined by the initial membrane potential, the strength of the synapses, and especially by the slope of the activation curve and the half activation voltage of the anomalous rectification. Increasing the half activation voltage, either directly or by changing the potassium equilibrium potential, will raise the number of synapses preferred by the neuron, and increase the voltage range over which synapses act cooperatively. If it becomes too positive, however, the strength of the cooperative effect is diluted by the powerful effect of the synaptic nonlinearity. Increasing the slope of the activation curve strengthens the cooperative effect, but at the expense of narrowing the range of synaptic densities over which the cooperative effect can be observed.

The current attenuating effect of dendritic spines is not required for this cooperative interaction between synapses, which can be seen with in simulations of axodendritic synapses as well. The reduced dendritic EPSP amplitudes obtained with current attenuating dendritic spines, however, increases the magnitude of the cooperative effect, and the preferred number of active synapses, as does decreasing the magnitude or duration of the synaptic conductance change.

Implications for Neostriatal Function:

One of the most obvious features of the neostriatal spiny neuron is its relative silence. Even in awake animals, these cells often fire only in rare episodes. Because the cells contain and release GABA, and because they have dense local axonal arborizations, much of the early work on neostriatal neurons concentrated on the idea that the silence of these cells is due to active inhibition generated within the neostriatum (e.g. Hull et al., 1973; Bernardi et al., 1975; 1976). More recent studies have failed to reveal this inhibition, and have suggested the opposite view, i.e. the neurons do not fire because they have insufficient excitatory synaptic input, despite the large number of excitatory synaptic contacts formed onto them by cortical and thalamic afferent fibers (Wilson and Groves, 1981; Wilson et al., 1983a; Wilson, 1986; Calabresi et al., 1990). If corticostriatal or thalamostriatal neurons fired very rarely there would be no paradox in this view, but this is not the case. Studies of corticostriatal neurons at least, show them to be spontaneously active under conditions in which neostriatal neurons are mostly silent (e.g. Landry et al., 1984; Cowan and Wilson, 1990). In addition, neostriatal spiny neurons have been shown to be chronically depolarized by 10-20 mV by tonic but subthreshold afferent synaptic activity (Wilson et al., 1983b).

These experiments suggested that neostriatal neurons do not lack synaptic input, but rather that individual synapses are so weak that large numbers of correlated synaptic inputs are required to depolarize the neuron sufficiently to fire action potentials (Wilson and Groves, 1981; Wilson et al., 1983b; Calabresi et al., 1990).

The reasons for the ineffectiveness of afferent synapses on the neostriatal spiny neurons remain unavailable for direct study. On the basis of the findings presented here, the current attenuation effect of dendritic spines, as previously suggested (Wilson, et al., 1983a) seems unlikely to be a large factor in determining the strength of the synapses in the neostriatum. Unless synaptic conductances on neostriatal neurons have unusually short durations or spine necks have unexpectedly high cytoplasmic resistances, this effect is not likely to account for much more than a 50% attenuation of EPSP amplitudes at the soma. A potentially larger effect may be due to the effect of the additional membrane of the dendritic spines on the effective electrotonic length of the dendrites, coupled with the strong anomalous rectification, which both lowers the overall input resistance of the neuron, and exaggerates the effects of the dendritic spines on the length constant. The reduction of input resistance in the dendrite would also promote the operation of dendritic spines as current attenuators. The current attenuation effect of dendritic spines requires conductance changes large enough to produce saturating EPSPs in the spine heads, and relies upon the low input impedance of the dendrite to insure that the local dendritic EPSP will be small. The linear model of the spiny neuron, combined with current estimates of the electrical characteristics of the spine membrane and cytoplasm, predicts that the EPSP generated from such an axospinous synapse on a neostriatal neuron would actually be quite large. That is, the input resistance of the dendrite is so high that saturating EPSPs in the spine head produce dendritic and somatic EPSP that are larger than would be consistent with neurophysiological data. If the conductance change is made small enough to get the appropriate-sized EPSP in the soma, it fails to produce a saturating EPSP in the spine, and the current attenuation effect is lost. This is similar to the situation described for hippocampal neurons, and which has led to the conclusion that dendritic spines probably do not substantially attenuate synaptic current in those cells (Turner, 1984; Harris and Stevens, 1989). In neostriatal neurons, the extremely low membrane resistivities generated by the fast inward rectifier can result in low enough dendritic input impedances to reconcile the simulations and the physiological data. Thus the relative ineffectiveness of individual afferent synapses in neostriatal neurons when the membrane potential is near its resting level can be accounted for by a combination of the fast inward rectifier, the short length constant of the spiny dendrite, and perhaps also the current attenuating effect of dendritic spines.

Dendritic spines have also been proposed to act to linearize synaptic interactions (see refs in Wilson, 1984). Because the spine neck acts as a series resistance between the conductance change on a dendritic spine head and the rest of the dendritic tree, a large conductance decrease in a spine head will not as effectively act to shunt currents generated elsewhere on the dendrites. In addition, the small dendritic EPSPs that are generated by axospinous synapses may reduce the effect of the classical synaptic nonlinearity. The possible effect of the spine neck resistance on synaptic shunting does not play a role when the interactions are between excitatory afferents with the same synaptic reversal potentials, as considered here. The effect on local dendritic EPSPs and thus the driving force for synaptic currents was large in the simulations of synchronous afferent synaptic activity, but only when the density of synaptic inputs was low. When axospinous synaptic inputs were closely spaced on the dendrite, either because they were clustered or because the overall level of synaptic input is large, the dendritic EPSPs became large enough to engage the synaptic nonlinearity. The difference between axospinous and axodendritic synapses was greatly reduced when the local density of activated synapses exceeded only a few percent of the density of afferent synapses present on the spiny neurons, and was practically absent with activation of 50% of the synapses. One result of this is that the effectiveness of synapses on the spiny neuron is greatly decreased if the synapses are spatially clustered on the dendrites. A single axon that makes several synaptic contacts on a neostriatal neuron will have a much greater potential for summing with other active inputs if it distributes its synapses as far apart as possible. Afferent fibers in the neostriatum probably do make spatially distributed synaptic

contacts, because they branch infrequently and make synapses en passant as they cross over the dendritic trees of the spiny neuron.

The dependence of the membrane resistance of the spiny neuron on membrane potential introduces the possibility for cooperative synaptic interactions. The conditions which favor this cooperative effect are: (1) widely distributed synaptic input, (2) adjustment of the activation curve of the inwardly rectifying conductance so that it is almost fully on at the potassium equilibrium potential and disengages over a range of potentials corresponding to the local (dendritic) amplitudes of the EPSPs that should interact cooperatively but is far from the reversal potential of the excitatory inputs, and (3) placement of the inwardly rectifying conductance on the dendrites. This latter condition is necessary because the effect of the inward rectification on dendritic length constant is critical to the synaptic cooperativity.

This cooperative effect among synapses may contribute to the existence of the episodic depolarizations that characterize the in vivo pattern of activity in neostriatal projection neurons. In the hyperpolarized state of the membrane that separates depolarizing episodes, the input resistance is low and the effect of an individual synaptic input is negligible. If there are correlated synaptic inputs distributed over the dendritic field, these can depolarize the neuron to some degree, raising the input resistance and decreasing the electrotonic distance between the interacting synapses. This will make the neuron more sensitive to these and other excitatory inputs. This positive feedback effect of the inward rectification will tend to give an abrupt onset and offset to episodes of synaptic depolarization, as has been reported for neostriatal neurons (Wilson et al. 1982). The number of active synapses required to produce a depolarizing episode would, according to this view, depend upon the activation curve for the inward rectification, the background level of unpatterned synaptic input present but not correlated with the inputs whose correlated activity will determine the timing of the episode, and the uniformity of the distribution of synaptic inputs whose activity is correlated. Thus the conductance responsible for the fast anomalous rectification in neostriatal neurons is well situated to adjust the sensitivity of the neostriatal neuron to different patterns of synaptic input and would make an ideal target for modulation by other neurotransmitters and peptides.

ACKNOWLEDGEMENTS

Supported by NIH grant NS20743 and ONR grant N00014-89-J-3179. High voltage electron microscopy supported by NIH grant RR00592 to the Laboratory for High Voltage Electron Microscopy at Boulder, Colorado. Thanks to Dr. D.J. Surmeier for thoughtful comments and helpful suggestions.

REFERENCES

Bargas, J., Galarraga, E. and Aceves, J. (1988). Electrotonic properties of neostriatal neurons are modulated by extracellular potassium. Brain Res. ,**72**, 390-398.

Bernardi, G., Marciani, M.G., Morocutti, C., Giacomini, P. (1975). The action of GABA on rat caudate neurones recorded intracellularly. Brain Res., **92**, 511-515.

Bernardi, G., Marciani, M.G., Morocutti, C. and Giacomini, P. (1976). The action of picrotoxin and bicuculline on rat caudate neurons inhibited by GABA. Brain Res., **102**, 397-384.

Brown, T.H., Chang, V.C., Ganong, A.H., Keenan, C.L. and Kelso, S.R. (1988). Biophysical properties of dendrites and spines that may control the induction and expression of long-term potentiation. Neurol. Neurobiol., **35**, 201-264.

Calabresi, P., Mercuri, N., Stanzione, P., Stefani, A. and Bernardi, G. (1987). Intracellular studies on the dopamine-induced firing inhibition of neostriatal neurons in vitro: evidence for D1 receptor involvement. Neuroscience, **20**, 757-771.

Calabresi, P., Mercuri, N.B., Stefani, A. and Bernardi, G. (1990). Synaptic and intrinsic control of membrane excitability of neostriatal neurons. I. An in vivo analysis. J. Neurophysiol., **63**, 651-662.

Cowan, R.L. and Wilson, C.J. (1990). Contralateral neostriatal and ipsilateral pyramidal tract stimulation produce synaptic responses in pyramidal tract and crossed corticostriatal neurons. Soc. Neurosci. Abst., **16**, 417.

Diamond, J., Gray, E.G. and Yasargil,G.M. (1970). The function of the dendritic spine: An hypothesis. In P. Andersen and J.K.S. Jansen (Eds) Excitatory Synaptic Mechanisms, Oslo; Universitet forlaget, pp. 213-222.

DiFiglia, M., Pasik, P., and Pasik, T. (1976). A Golgi study of

neuronal types in the neostriatum of monkeys. Brain Res., **114**, 245-256.

Chang, H.T., Wilson, C.J.and Kitai, S.T. (1981). Single neostriatal efferent axons in the globus pallidus: A light and electron microscopic study. Science, **213**, 915-918.

Durand, D. (1984). The somatic shunt cable model for neurons. Biophys. J., **46**, 645-653.

Evarts, E.V., Kimura, M., Wurtz, R.H. and Hikosaka, O. (1984). Behavioral correlates of activity in basal ganglia neurons. Trends. Neurosci., **7**, 447-453.

Fleshman, J.W., Segev, I., Cullheim, S. and Burke, R.E. (1983). Matching electrophysiological measurements in cat motoneurons. Neurosci. Abst., **9**, 341.

Hagiwara, S. and Takahashi, K. (1974). The anomalous rectification and cation selectivity of a starfish egg cell. J. Membrane Biol., **18**, 61-80.

Harris, K.M. and Stevens, J.K. (1989). Dendritic spines of CA1 pyramidal cells in the rat hippocampus: Serial electron microscopy with reference to their biophysical characteristics. J. Neurosci., **9**, 2982-2997.

Hull, C.D., Bernardi, G. and Buchwald, N.A. (1970). Intracelluar responses of caudate neurons to brain stem stimulation. Brain Res., **22**, 163-179.

Hull, C.D., Bernardi, G., Price, D.D. and Buchwald, N.A. (1973). Intracellular responses of caudate neurons to temporally and spatially combined stimuli. Exp. Neurol., **38**, 324-336.

Kawaguchi, Y., Wilson, C.J. and Emson, P.C. (1990a). Intracellular recording of identified neostriatal patch and matrix spiny cells in a slice preparation preserving cortical inputs. J. Neurophysiol., **62**, 1052-1068.

Kawaguchi, Y., Wilson, C.J. and Emson, P.C. (1990b). Projection subtypes of rat neostriatal matrix cells revealed by intracellular injection of biocytin. J. Neurosci., **10**, 3421-3438.

Kawato, M. (1985). Cable properties of a neuron model with non-uniform membrane resistivity. J. Theor. Biol., **111**, 149-169.

Kawato, M., Hamaguchi, T., Murakami, F. and Tsukahara, N. (1984). Quantitative analysis of electrical properties of dendritic spines. Biol. Cybern., **50**, 447-454.

Kita, T., Kita, H. and Kitai, S.T. (1984). Passive electrical membrane properties of rat neostriatal neurons in an in vitro slice preparation. Brain Res., **300**, 129-139.

Koch, C. and Poggio, T. (1984). A theoretical analysis of electrical properties of spines. Proc. R. Soc. Lond. B, **218**, 455-477.

Landry, P., Wilson, C.J. and Kitai, S.T. (1984). Morphological and electrophysiological characteristics of pyramidal tract neurons in the rat. Exp. Brain Res., **57**, 177-190.

Mastronarde, D.N., Wilson, C.J., and McEwen, B. (1989). Three dimensional structure of intracellularly stained neurons and their proceses revealed by HVEM and axial tomography. Soc. Neurosci. Abst., **15**, 256.

Miller, J.P., Rall, W. and Rinzel, J. (1985). Synaptic amplification by active membrane in dendritic spines. Brain Res., **325**, 325-330.

Perkel, D.H. and Perkel, D.J. (1985). Dendritic spines: Role of active membrane in modulating synaptic efficacy. Brain Res., **325**, 331-335.

Rall, W. (1977). Core conductor theory and cable properties of neurons. In J.M. Brookhart, V.B. Mountcastle and E.R. Kandel (Eds.) Handbook of Physiology Sect. 1 Vol. 1. , Bethesda MD; American Physiological Society pp. 39-97.

Rall, W. (1974). Dendritic spines, synaptic potency and neuronal plasticity. In: Cellular Mechanisms Subserving Changes in Neuronal Activity. C.D. Woody, K.A. Brown, T.J. Cros and J.D. Knispel, (Eds) Brain Information Service UCLA, Los Angeles, pp. 13-21.

Rall, W. and Segev, I. (1988). Synaptic integration and exictable dendritic spine clusters: Structure/function. Neurol. Neurobiol., **37**, 263-282.

Sedgwick, E.M. and Williams, T.D. (1967). The response of single units in the caudate nucleus to peripheral stimulation J. Physiol. (Lond.), **189**, 281-298.

Shepherd, G.M., Brayton, R.K., Miller, J.P., Segev, I., Rinzel, J. and Rall, W. (1985). Signal enhancement in distal cortical dendrites by means of interactions between active dendritic spines. Proc. Natl. Acad. Sci. USA, **87**, 2192-2195.

Sugimori, M., Preston, R.I. and Kitai, S.T. (1978) Response properties and electrical constants of caudate neurons in the cat. J. Neurophysiol., **41**, 1662-1675.

Surmeier, D.J., Bargas, J. and Kitai, S.T. (1988). Voltage-clamp analysis of a transient potassium current in rat neostriatal neurons. Brain Res., **473**, 187-192.

Surmeier, D.J., Bargas, J. and Kitai, S.T. (1989). Two types of A-current differing in voltage dependence are expressed by neurons of the rat neostriatum. Neurosci. Lett., **103**, 331-337.

Surmeier, D.J., Stefani, A., Foehring, R.C. and Kitai, S.T. (1991) Developmental regulation of a slowly-inactivating potassium conductance in rat neostriatal neurons. Neurosci. Lett., **122**, 41-46.

Turner, D.A. (1984). Conductance transients onto dendritic spines in a segmental cable model of hippocampal neurons. Biophys. J., **46**, 85-96.

Wilson, C.J. (1984). Passive cable properties of dendritic spines and spiny neurons. J. Neurosci. 4, 281-297.

Wilson, C.J. (1986). Postsynaptic potentials evoked in spiny neostriatal projection neurons by stimulation of ipsilateral or contralateral neocortex. Brain Res., **367**, 201-213.

Wilson, C.J. (1987). Three dimensional analysis of neuronal geometry using HVEM. Journal of Electron Microscopic Technique, **6**, 175-183.

Wilson, C.J. and Groves, P.M. (1980). Fine structure and synaptic connections of the common spiny neuron of the rat neostriatum. A study employing intracellular injection of horseradish peroxidase. J. Comp. Neurol., **194**, 599-615.

Wilson, C.J. and Groves, P.M. (1981). Spontaneous firing patterns of identified spiny neurons in the rat neostriatum. Brain Res., **220**, 67-80.

Wilson, C.J., Chang, H.T. and Kitai, S.T. (1982). Origins of postsynaptic potentials evoked in identified rat neostriatal neurons by stimulation in substantia nigra. Exp. Brain Res. ,**45**, 157-167.

Wilson, C.J., Chang, H.T. and Kitai, S.T. (1983a). Disfacilitation and long lasting inhibition of neostriatal neurons in the rat. Exp. Brain Res., **51**, 217-226.

Wilson, C.J., Groves, P.M., Kitai, S.T. and Linder, J.C. (1983b). Three-dimensional structure of dendritic spines in the rat neostriatum. J. Neurosci., **3**, 383-398.